Research Article | Vol. 9, No. 4 | 1 Apr 2019 | OPTICAL MATERIALS EXPRESS 1583
Optical Materials EXPRESS

Producing true-color rainbows with patterned multi-layer liquid-crystal polarization gratings

FRANS SNIK,[1,2,*] MICHIEL RODENHUIS,[2] MICHAEL J. ESCUTI,[3] LEANDRA BRICKSON,[3] KATHRYN HORNBURG,[3] JIHWAN KIM,[3] CHRIS KIEVID,[4] SEBASTIAAN GROENHUIJSEN,[4] AND DAAN ROOSEGAARDE[4]

[1]*Leiden Observatory, Leiden University, P.O. Box 9513, 2300 RA Leiden, The Netherlands*
[2]*NOVA, P.O. Box 9513, 2300 RA Leiden, The Netherlands*
[3]*Department of Electrical and Computer Engineering, North Carolina State University, Raleigh, NC, 27695, USA*
[4]*Studio Roosegaarde, Vierhavensstraat 52-54, 3029 BG Rotterdam, The Netherlands*
[*]*snik@strw.leidenuniv.nl*

Abstract: We present the technical design of the art installation Rainbow Station, that projects a 40-m diameter true-color rainbow. The core technology is comprised of a patterned polarization grating that produces the rainbow with the correct shape and correct color order. We achieve an effective grating period as small as 1.55 μm, and obtain high diffraction efficiency over the entire visible spectral range thanks to a multi-layer liquid-crystal implementation. The -1 spectral order is suppressed by circular polarization filtering.

1. Introduction

Rainbows have been prevalent throughout the entire history of art, and many (positive) attributes are associated with them [1]. However, in most cases it is impossible to achieve a true-color representation of the colors of a rainbow, unless actual refraction (e.g. in rain droplets) or diffraction of white light is implemented. At the end of 2014, our collaboration, led by Studio Roosegaarde, designed, tested, and constructed the art installation Rainbow Station (see https://www.studioroosegaarde.net/project/rainbow-station) at the Amsterdam Central train station in the Netherlands. During 2015, the International Year of Light, a true-color rainbow could be observed on the east face of the monumental, large arch construction from 1889 that spans over the first three platforms. This rainbow, like actual rainbows in nature, only presented itself for a few minutes at an unpredictable time. Contrary to rainbows in nature, the rainbow of Rainbow Station only appeared after sunset.

The main technical challenges for this art installation were:

1. The rainbow shall follow the exact shape of the ~40-m wide train station arch;
2. The rainbow shall exhibit true colors, i.e., no RGB projection;
3. The sequence of colors shall be clearly distinguishable, and in the right order (i.e., red up);
4. The efficiency across the visible range shall be high and uniform;
5. Any light leaking in other directions shall be suppressed.

We very quickly came to the conclusion that existing solutions using (conical) prisms and classical gratings all yielded unsatisfactory results. We therefore implemented brand-new liquid-crystal technology, in combination with a novel diffraction concept to accomplish the artistic vision. The so-called "polarization grating" [2–4] consists of a flat substrate, with flat

#352531 https://doi.org/10.1364/OME.9.001583
Journal © 2019 Received 21 Nov 2018; revised 24 Jan 2019; accepted 28 Jan 2019; published 6 Mar 2019

Optical Materials EXPRESS

liquid-crystal layer deposited on top. These liquid crystals are birefringent, and are patterned such that their fast axes exhibit a continuous rotation in a particular direction, which becomes the direction of diffraction. Contrary to classical gratings, polarization gratings utilize the geometric phase [5], also know as the Pancharatnam [6]–Berry [7] phase. The diffraction efficiency is maximal when then liquid-crystals constitute a half-wave retarder. Such geometric-phase holograms operate on circular polarization states, which flip handedness upon traversing through the element. In addition, the light accrues a geometric phase pattern $\delta_{\pm}$ on the optical footprint coordinates (u, v) cf.:

$$\delta_{\pm}(u, v) = \pm 2 \cdot \Phi(u, v), \tag{1}$$

in which $\Phi(u, v)$ denotes the pattern of liquid-crystal fast-axis orientations.

The geometric phase has an opposite phase for the left/right-handed circular polarization, described here by the ± sign. Moreover, the wavelength is completely absent in Eq. (1), and geometric-phase holograms are therefore strictly achromatic. However, if the liquid-crystal layers have a retardance offset from half-wave, a leakage term emerges that carries a small fraction of light that does not flip handedness and does not undergo diffraction. Thanks to multi-layer liquid crystal optimization, polarization gratings (and other such geometric-phase optical elements) can achieve an achromatized retardance behavior as a function of wavelength, and thus achieve very large spectral bandwidths ($\lambda/\Delta\lambda \approx 100\%$) over which the diffraction efficiency in orders ±1 approaches 2·50%, and the leakage term only typically contains ∼1% of the light [2, 8]. As the geometric phase is applied very locally, no higher orders than ±1 emerge [5]. Furthermore, through a direct-write technique of an alignment layer, virtually *any* phase pattern can be implemented on a substrate, as all the liquid-crystal layers self-align to the written pattern, which has a resolution of ∼2 μm [9].

In recent years, we have introduced this revolutionary technology in astronomical instrumentation. A first implementation comprised the use of a polarization grating to provide spectropolarimetric imaging of heavenly bodies [10]. Currently, we are designing and commissioning many so-called coronagraphic optics based on patterned liquid crystals, which serve to selectively suppress the diffractive halo of starlight, such that we can observe faint exoplanets that orbit nearby stars [11]. The big final goal of this research is to make images of Earth-like exoplanets, and find signs of habitability or even of habitation in their (integrated) light. A first important step would be the unambiguous detection of the presence of liquid water (a prerequisite for life, at least life as we know it). Therefore, we are literally hunting for (polarized) rainbows on exoplanets, as they are a clear indicator for liquid water [12]. All in all, many reasons to adopt the patterned multi-layer liquid crystal technology to produce the rainbow of Rainbow Station.

2. Design

2.1. Geometrical design

The novel concept for this custom polarization grating design is introduced in Fig. 1. The grating phase pattern consists of concentric rings with an outward geometric phase ramp for diffraction order +1, enabled by a continuously rotating liquid-crystal axis. The grating consists of two parts (top + bottom), that both produce the same far-field diffraction in the same order.

We describe the rainbow pattern and consequently the grating/hologram pattern in polar coordinates. We start wth a 3D model of the Amsterdam train station, and trace the outline $R(\theta)$ as seen from the location of the projection tower for the reddest wavelength (700 nm) onto the station's arch at ∼40 m distance. We fit a simple polynomial equation to 19 discrete points to obtain a smooth function. Note that this function is not constant as the position at which the light is projected out of the projection tower is not concentric with the greater arc of the arch, and the function is even not left/right-symmetric as the projection tower had to be located in the middle of a platform, that is not in the middle of the arch. Through the grating equation, we translate the

Optical Materials EXPRESS

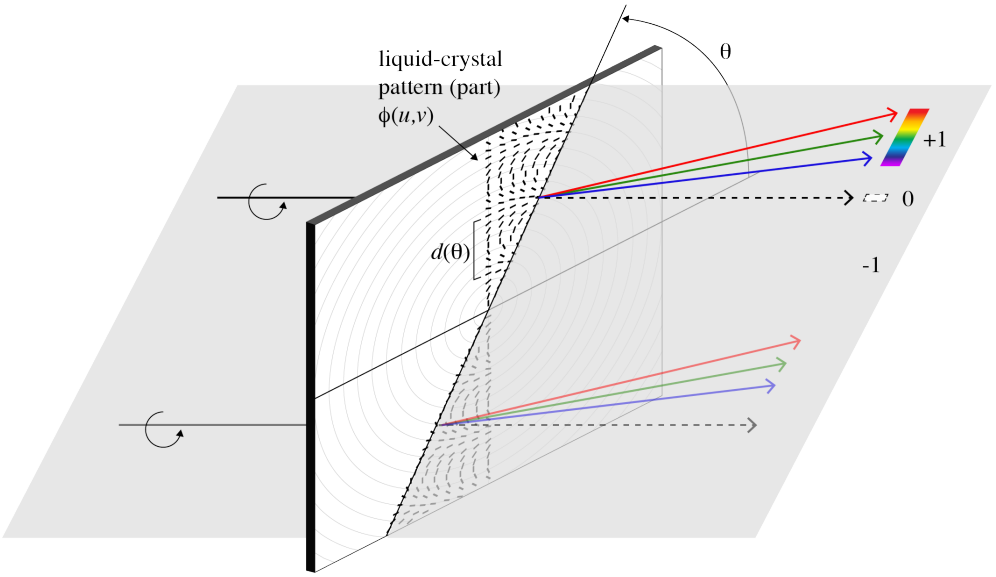

Fig. 1. Schematic representation of the patterned polarization grating used for Rainbow Station. The rings represent lines of constant fast-axis orientation (only two slices of liquid crystal orientations are drawn), and hence geometric phase. The diffraction for only right-handed input polarization is shown for a single direction θ in polar coordinates. For a perfect half-wave retardance, all light will produce an arced rainbow pattern in order +1. Note that there is a discontinuity between the top and bottom parts, as otherwise the lower part would diffract downward. In practice, a small fraction of light will be present in the leakage term (order 0), and, in case of imperfect circular polarization filtering, in order -1.

required shape of the rainbow into the corresponding grating period $d(\theta)$ for each direction θ. We perform a Fraunhofer propagation for the grating thus obtained (including the two separate parts) for a single wavelength, and found a slight mismatch with the target shape at locations with a steep gradient in $R(\theta)$. We therefore applied a single iteration to the above procedure, and thus obtain the final grating/hologram design. Through Eq. (1) the design is converted into the liquid-crystal pattern $\Phi(u, v)$. Note this procedure can be applied to obtain any $R(\theta)$ rainbow shape, including straight lines.

2.2. Liquid-crystal film design and manufacturing

The hologram design led to grating periods ranging from 1.55 μm for the widest points on the sides of the rainbow to 2.34 μm for the apex. In order to realize these small spatial frequencies, which lead to relatively large (in 2014) diffraction angles for achromatic holograms of nearly 20°, we employed two techniques to help us. First, we applied a hologram replication principle [13,14], via contact lithography, to make a mask at larger periods for which the grating periods were all reduced by half for each replication. Second, we arranged two identical holograms face-to-face to once more effectively reduce by half the grating periods. Unlike regular gratings for which the light in order +1 of the first grating would be distributed over orders ±1 of the second grating, polarization gratings maintain complete diffraction directionality for both circular polarization states. Therefore, in order to achieve the effective grating periods of 2.34 to 1.55 μm in the final parts, we began with a mask with periods in the range of 37.4 to 24.8 μm. This was then replicated three times to achieve a replica hologram "half" with a range of 4.7 to 3.1 μm. Finally,

Optical Materials EXPRESS

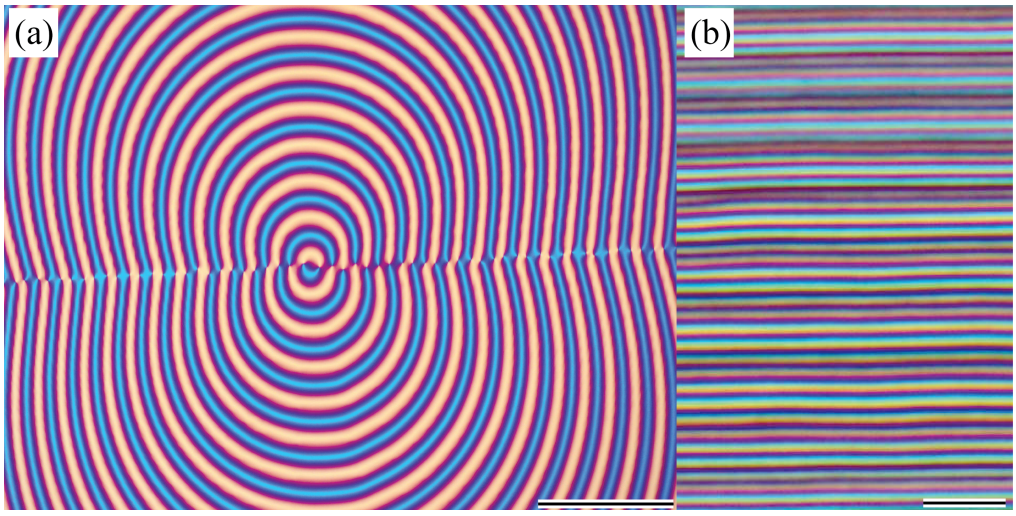

Fig. 2. Polarized microscope image of the holograms used for Rainbow Station: (a) the mask, taken at the center of the hologram, with scale bar indicating 200 μm, and (b) the replica, taken near an edge, with scale bar indicating 20 μm. In this particular orientation configuration of the polarizers and the liquid-crystal structure, the grating appears sinusoidal instead of having a continuous phase ramp.

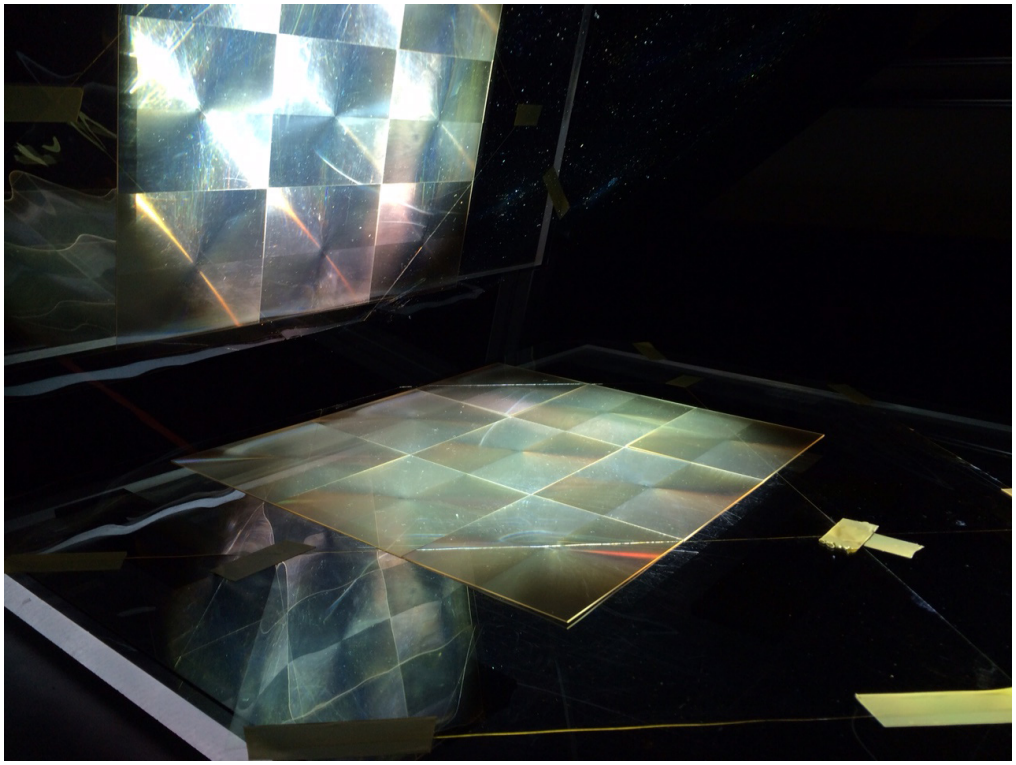

Fig. 3. Photo of the polarization and diffractive optics that form the heart of the Rainbow Station installation. On top of a glass plate is a stack of, respectively, polarizer foil, quarter-wave retarder foil, and the 3×3 mosaic of polarization gratings. On the top the large fold mirror is used to steer the diffracted beam in the right direction.

Optical Materials EXPRESS

by laminating two of these "halves", the necessary small periods were effectively implemented.

We used a photo-alignment layer (LIA-CO01, DIC Corp, 30 nm thick) [15] to achieve the inhomogeneous profile of the liquid crystal optic axis [2, 16] in the mask. We used a direct-write scanning system [9, 16] to create the orientation pattern in the 15×15 cm^2 mask, with a fluence of about 1 J/cm^2. A polarizing optical microscope was used to image the center of the hologram, shown in Fig. 2(a). After this pattern was replicated [13, 14], the periods were reduced in size. An image of the resulting replica near the edge is shown in Fig. 2(b). In order to realize the achromatic retardance spectra for high diffraction efficiency from 400 to 700 nm range, we created the two-layer liquid crystal polymer structure introduced in Ref. [2]. After lamination, the glass plates were diced down to 11×11 cm^2 size. We produced nine tiles of this hologram to enable a 3×3 tiling that covers the footprint of the projector light beam.

2.3. Projector design

The white light source to produce the rainbow is a 4 kW metal halide "followspot", which is installed vertically inside the projector tower. The lamp has a fairly uniform spectral flux over the visible spectrum following the black-body spectrum of the sun, with a number of emission lines at roughly double the intensity. The illumination system has a 2° divergence. Above the light source, the 3×3 tiles gratings and associated polarization optics are stacked and aligned on top of a glass plate, and cover most of the beam diameter of ~35 cm, see Fig. 3. To only select one circular polarization state, the light is first linearly polarized by a large polarizer foil (Edmund Optics 86-200), and consecutively turned into circular polarization with a mosaic of quarter-wave retarder foils (Edmund Optics 88-253) oriented at 45° with respect to the polarizer. Note that this polarizer absorbs quite some power (> 50%) from the unpolarized light source. Given the spectral irradiance at the position of the liquid-crystal elements and the absorption properties of the utilized liquid-crystal materials, we estimate a total lifetime of >30 years, assuming that the installation produces one rainbow per day for the duration of 10 minutes. The final optical element is a large folding mirror, which 2D orientation is fine-tuned to align the projected rainbow with the station's arch.

3. Performance

A photographic impression of the rainbow as it was visible during 2015 is shown in Fig. 4. Note that an RGB color image can never do the full gamut of a true-color rainbow any justice. It is clear that the rainbow indeed follows the shape of the arch nicely, and that the full spectrum is represented in a visually pleasing wide band. The exact appearance of the rainbow obviously depends on the structure that is projected onto, and more specifically its spectral Bidirectional Reflectance Distribution Function (BRDF). In this case, we get by far the largest color response from the window panes that are painted white. The actual windows in between are dirty enough such that the rainbow is also visible from inside the arch due to scattering on dust particles. However, the ambient illumination due to "street lights" is much stronger inside the arch than outside, so the encounter with the rainbow is more powerful outside than inside.

Fig. 5 shows the measured zero-order transmittance of one of the tiles (after the two "halves" were laminated), where $T_0 = 1.2\%$ on average across the visible range. The total first-order transmittance was estimated as $\Sigma T_{\pm 1} = 96\% - T_0$, also shown, which includes the loss from the anti-reflection coatings on the outside faces of the glass. We can therefore estimate $\Sigma T_{\pm 1} = 94.8\%$ on average. We indeed found that the polarization optics in the projection tower did a good job of suppressing the -1 order. We blocked the zero-order leakage with a simple plate in front of the tower.

Optical Materials EXPRESS

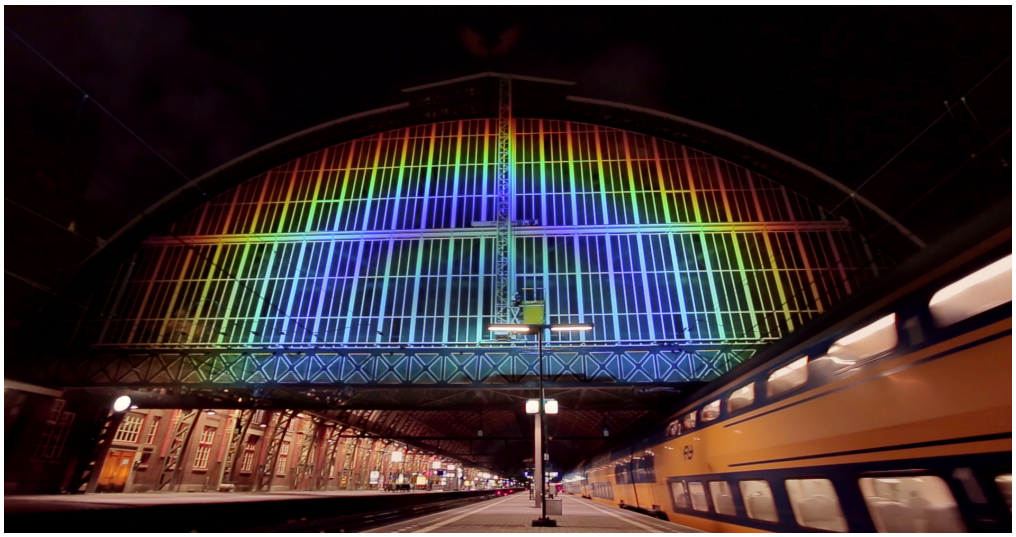

Fig. 4. The rainbow of Rainbow Station as seen in front of the projector tower. Photo credit: Studio Roosegaarde.

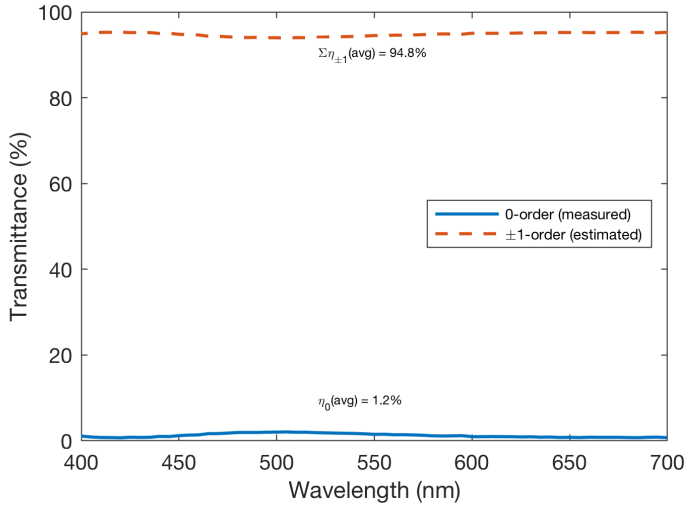

Fig. 5. Measured zero-order transmittance and estimated total first-order transmittance of the installed replica holograms.

4. Conclusion

Although the artistic appearance is quite distinct, it took a significant amount of research and development to produce the rainbow of Rainbow Station. After its operation in 2015, we are currently planning to have similar rainbows appear in special locations all over the world. Usually, the technologies behind similar art works remain hidden as only the experience is ultimately of importance, and knowledge of its inner workings would "demystify" them. In this particular case we feel strongly that explaining the technical development and scientific context, as presented in this paper, really adds interesting layers of significance to the artwork.

Optical Materials EXPRESS

Acknowledgements

We thank ImagineOptix Corp. and ColorLink Japan, Ltd., for assistance in manufacturing the liquid crystal geometric-phase holograms.

Funding

European Research Council (ERC) Starting Grant (678194; FALCONER).

References

1. R. L. Lee and A. B. Fraser, *The Rainbow Bridge: Rainbows in Art, Myth, and Science* (Penn State Press, 2001).
2. C. Oh and M. J. Escuti, "Achromatic diffraction from polarization gratings with high efficiency," Opt. Lett. **33**, 2287–2289 (2008).
3. C. Packham, M. Escuti, J. Ginn, C. Oh, I. Quijano, and G. Boreman, "Polarization gratings: A novel polarimetric component for astronomical instruments," Publ. Astron. Soc. Pac. **122**, pp. 1471–1482 (2010).
4. L. Nikolova and T. Todorov, "Diffraction efficiency and selectivity of polarization holographic recording," Opt. Acta **31**, 579–588 (1984).
5. M. J. Escuti, J. Kim, and M. W. Kudenov, "Controlling light with geometric-phase holograms," Opt. Photon. News **27**, 22–29 (2016).
6. S. Pancharatnam, "Generalized theory of interference, and its applications. part i. coherent pencils," Proc. Indian Acad. Sci. Sect. A **44**, 247–262 (1956).
7. M. V. Berry, "Quantal Phase Factors Accompanying Adiabatic Changes," Royal Soc. Lond. Proc. Ser. A **392**, 45–57 (1984).
8. R. K. Komanduri, K. F. Lawler, and M. J. Escuti, "Multi-twist retarders: broadband retardation control using self-aligning reactive liquid crystal layers," Opt. Express **21**, 404–420 (2013).
9. M. N. Miskiewicz and M. J. Escuti, "Direct-writing of complex liquid crystal patterns," Opt. Express **22**, 12691–12706 (2014).
10. M. Rodenhuis, F. Snik, G. van Harten, J. Hoeijmakers, and C. U. Keller, "Five-dimensional optical instrumentation: combining polarimetry with time-resolved integral-field spectroscopy," in *Polarization: Measurement, Analysis, and Remote Sensing XI,* vol. 9099 of *Proc. SPIE* (2014), p. 90990L.
11. F. Snik, G. Otten, M. Kenworthy, M. Miskiewicz, M. Escuti, C. Packham, and J. Codona, "The vector-APP: a broadband apodizing phase plate that yields complementary PSFs," in *Modern Technologies in Space- and Ground-based Telescopes and Instrumentation II,* vol. 8450 of *Proc. SPIE* (2012), p. 84500M.
12. T. Karalidi, D. M. Stam, and J. W. Hovenier, "Looking for the rainbow on exoplanets covered by liquid and icy water clouds," Astron. Astrophys. **548**, A90 (2012).
13. M. J. Escuti, "Methods of fabricating liquid crystal polarization gratings on substrates and related devices," US Pat. Appl. **60/912,036** (2007).
14. S. R. Nersisyan, N. V. Tabiryan, D. M. Steeves, and B. R. Kimball, "Characterization of optically imprinted polarization gratings," Appl. Opt. **48**, 4062–4067 (2009).
15. V. G. Chigrinov, V. M. Kozenkov, and H.-S. Kwok, *Photoalignment of liquid crystalline materials: physics and applications*, vol. 17 (John Wiley & Sons, 2008).
16. J. Kim, Y. Li, M. N. Miskiewicz, C. Oh, M. W. Kudenov, and M. J. Escuti, "Fabrication of ideal geometric-phase holograms with arbitrary wavefronts," Optica **2**, 958–964 (2015).